The cytosolic *Arabidopsis thaliana* cysteine desulfurase ABA3 delivers sulfur to the sulfurtransferase STR18

Benjamin Selles[1], Tiphaine Dhalleine[1], Mathilde Hériché[1,2], Nicolas Rouhier[1], Jérémy Couturier[1]*

[1] Université de Lorraine, INRAE, IAM, F-54000 Nancy, France.

Present address: [2] Agroécologie, AgroSup Dijon, CNRS, Université de Bourgogne, INRAE, Université de Bourgogne Franche-Comté, F-21000 Dijon, France

*Corresponding author: Jérémy Couturier

Email: jeremy.couturier@univ-lorraine.fr

Running title: ABA3 provides sulfur to STR18

Keywords: cysteine, cysteine desulfurase, sulfurtransferase, trans-persulfidation reaction, rhodanese, sulfur trafficking

ABSTRACT

The biosynthesis of many sulfur-containing biomolecules depends on cysteine as a sulfur source. Cysteine desulfurase (CD) and rhodanese (Rhd) domain-containing protein families participate in the trafficking of sulfur for various metabolic pathways in bacteria and human. However, their connection is not yet described in plants even though the existence of natural chimeric proteins containing both CD and Rhd domains in specific bacterial genera suggests that the interaction between both proteins should be universal. We report here the biochemical relationships between two cytosolic proteins from *Arabidopsis thaliana*, a Rhd domain containing protein, the sulfurtransferase 18 (STR18), and a CD isoform, ABA3, and compare these biochemical features to those of a natural CD-Rhd fusion protein from the bacterium *Pseudorhodoferax sp.*. We found that the bacterial enzyme is bifunctional exhibiting both CD and STR activities using L-cysteine and thiosulfate as sulfur donors. *In vitro* activity assays and mass spectrometry analyses revealed that STR18 stimulates the CD activity of ABA3 by recovering the intermediate persulfide on its catalytic cysteine. The ability of STR18 to catalyze trans-persulfidation reactions from ABA3 to a reduced roGFP2 used as a model acceptor protein reveals that the ABA3-STR18 couple may represent an uncharacterized pathway of sulfur trafficking in the cytosol of plant cells, independent of ABA3 function in molybdenum cofactor maturation.

Sulfur is an essential macronutrient playing pivotal roles in the physiology and development of all organisms as it is present in cysteines and methionines but also in many other molecules such as sulfolipids, thionucleosides, vitamins (thiamin, biotin, lipoic acid) and in iron-sulfur (Fe-S) clusters or molybdenum cofactors (Moco) (1). In plants, cysteine is synthesized *via* the reductive assimilation of sulfate, before its conversion to methionine. It serves also as a building-block for glutathione biosynthesis and as the source of sulfur for the biosynthesis of most sulfur-containing cofactors or molecules mentioned above (1).

The cysteine desulfuration step is catalyzed by pyridoxal 5'-phosphate (PLP)-dependent cysteine desulfurases (CDs) and leads to the formation of a persulfide group on a catalytic cysteine and the concomitant release of alanine (2). The NifS protein from *Azotobacter vinelandii* was the first CD characterized for its involvement in the maturation of the complex Fe-S clusters present in nitrogenase (3). This functional assignment led to the subsequent identification of the IscS paralog, that serves as a general

system for the maturation of other Fe-S proteins but also for providing sulfur present in other molecules (4). In addition to IscS, *Escherichia coli* possesses two other CD isoforms, namely SufS and CsdA (5, 6). Bacterial and eukaryotic CDs share a similar fold and assemble as dimers but two groups have been distinguished based on distinct structural differences and reactivities (6). IscS- and NifS-like proteins are members of group I. They contain a 12-residue insertion in an exposed loop containing the catalytic cysteine. In *Ec*IscS, this extension is sufficiently flexible to allow the direct transfer of sulfur to multiple biological partners (7). SufS- and CsdA-like proteins belong to the group II and the loop containing the catalytic cysteine is shorter (8, 9). For this reason, they form a two-component system with specific activators/sulfur acceptors, *i.e.* *Ec*SufE and *Ec*CsdE with *Ec*SufS and *Ec*CsdA respectively, or SufU with SufS in *Bacillus subtilis* (10–13).

In plants, NFS1 (group I) and NFS2 (group II) are the CDs providing the sulfur required for Fe-S cluster assembly in mitochondria and chloroplasts, respectively (14, 15). The CD activity of NFS2 is relatively low in the absence of the specific SUFE1-3 activators (16–18) A third CD isoform, ABA3, is localized in the cytosol of plants. It is not involved in the maturation of cytosolic Fe-S proteins (the sulfur required is provided by the mitochondrial NFS1) but in Moco sulfuration, participating in the activation of aldehyde oxidase (AO) and xanthine dehydrogenase (XDH), two Moco-containing enzymes involved in abscisic acid biosynthesis and in purine degradation respectively (19, 20). ABA3 is formed by two domains, an N-terminal aminotransferase class V domain (InterPro: IPR000192) responsible for the CD activity, as in NFS1 and NFS2, fused to a C-terminal MOSC domain (InterPro: IPR005302 and IPR005303). The persulfide formed on the catalytic cysteine of the CD domain is transferred to a second cysteine present in the MOSC domain before the sulfur atom is finally incorporated into the Moco precursor (20, 22).

Similar trans-persulfidation reactions between CDs and other sulfur carrier proteins operate during the biosynthesis of sulfur-containing molecules. Among these sulfur carrier proteins are sulfurtransferases (STRs), widespread enzymes found in bacteria, archaea and eukarya. They possess a characteristic rhodanese (Rhd) domain usually containing a conserved reactive catalytic cysteine present in a specific Cys-X-X-Gly-X-Arg signature (23, 24). This cysteine is mandatory to the ability of STRs to catalyze trans-persulfidation reactions between a donor and an acceptor by forming themselves a cysteine persulfide as an intermediate. Three different STR classes have been defined with respect to their modular organizations and substrate specificities (23–25). STRs with a single Rhd domain use preferentially thiosulfate as a sulfur donor *in vitro* and are referred to as thiosulfate-STRs (TSTs, InterPro: IPR001307). Those possessing two Rhd domains use preferentially 3-mercaptopyruvate (3-MP) as a sulfur donor *in vitro* and were named 3-mercaptopyruvate (3-MP)-STRs (MSTs, InterPro: IPR036873). Only the C-terminal Rhd domain possesses a catalytic cysteine residue. Additional STR proteins contain one Rhd domain fused to one or several protein domains with another function conferring them specific roles (23, 24).

Examples of interaction between CDs and STRs in non-plant organisms has suggested a central hub function for CD/STR couples as sulfide/sulfur moieties are required for various metabolic pathways. In *E. coli*, the sulfur transfer from IscS to STR proteins, ThiI or YnjE, is involved in thiamine biosynthesis or in tRNA thiolation and Moco biosynthesis respectively (26, 27). A similar sulfur relay system exists in the cytosol of yeast and human. The human STR isoform, TUM1, participates in the biosynthesis of Moco cofactor, receiving sulfur from NFS1 (28). Moreover, TUM1 proteins ensure sulfur transfer to another STR isoform, referred to as Uba4 in yeast or CNX5 in human, playing a role in tRNA thio-modification (29).

Such sulfur transfer relays should be universal considering the existence of natural chimeric proteins containing both CD and Rhd domains in specific bacterial genera. However, their properties have not been characterized, nor the existence of a comparable system in plants. Previous studies on plant CDs were mostly focused on their role in Fe-S cluster biogenesis (NFS1, NFS2) and Moco sulfuration (ABA3), not on a possible interaction with STRs (14, 15, 21). Hence, we have investigated the biochemical properties and interactions between the *Arabidopsis thaliana* cytosolic ABA3 and STR18 and

compared these biochemical features to those of a natural CD-Rhd fusion protein encoded by the *Pseudorhodoferax sp.* bacterial genome. We demonstrated that the bacterial enzyme is bifunctional exhibiting both CD and thiosulfate-dependent STR activities. Concerning plant proteins, *in vitro* activity assays and mass spectrometry analyses revealed that STR18 stimulates the CD activity of ABA3 by efficiently reducing the persulfide formed on the CD catalytic cysteine. Using reduced roGFP2 as a model acceptor protein, we showed the ability of STR18 to catalyze trans-persulfidation reactions from ABA3 to roGFP2. These data suggest that the ABA3-STR18 couple represents a new pathway of sulfur trafficking in the cytosol of *A. thaliana*.

RESULTS

The natural CD-Rhd fusion protein of Pseudorhodoferax sp. is a bifunctional enzyme

Genomic analyses (gene clustering, gene co-occurrence, gene fusion) are powerful to predict functional associations. For instance, the existence of natural fusions in some organisms often reflects a functional interaction in other organisms in which the constituting protein domains are expressed as separate proteins. By interrogating the STRING database (https://string-db.org/) using the COG1104 specific to CDs, we have noticed the existence of both adjacent CD and Rhd genes and of natural CD-Rhd fusion genes/proteins in several bacteria. We focused our attention on a CD-Rhd isoform from *Pseudorhodoferax sp.* Leaf274. The catalytic cysteine residue usually conserved in each protein domain is present suggesting that this protein should possess both cysteine desulfurase and sulfurtransferase activities (Fig. 1A) (8, 23). The corresponding His-tagged recombinant protein exhibited a yellow color after purification. The UV-visible absorption spectrum exhibited an absorption band at 418 nm characteristic of the presence of a bound-PLP cofactor as in characterized CDs (Fig. 1B) (9). Analytical gel filtration analysis demonstrated that CD-Rhd eluted predominantly in a peak corresponding to an apparent volume/molecular mass of 108 kDa (Fig. 1C). From the theoretical molecular mass of CD-Rhd (54 kDa), we concluded that this protein formed homodimers as observed for other CDs (7, 8).

We have then evaluated the capability of the fusion protein to use L-cysteine or thiosulfate and determined the kinetic parameters of the reactions. The CD activity (*i.e.* cysteine desulfuration with the concomitant formation of a persulfide on catalytic cysteine) was monitored by measuring the release of H_2S from the persulfidated protein in the presence of chemical or physiological reducing acceptors (Fig. 1D). Catalytic efficiencies (k_{cat}/K_m) of 1.1 x 10^4 M^{-1} s^{-1}, 1.5 x 10^3 M^{-1} s^{-1} and 5.2 x 10^3 M^{-1} s^{-1} have been measured in the presence of DTT, reduced glutathione (GSH) and β-mercaptoethanol, respectively (Table 1), thus validating the CD activity of the fusion. The activity of the Rhd domain was also evaluated by monitoring the release of H_2S in the presence of DTT but providing thiosulfate as the canonical substrate of TST-type STRs instead of L-cysteine. The catalytic efficiency of the reaction was 5.4 x 10^3 M^{-1} s^{-1} and the apparent K_m value for thiosulfate was 331 ± 70 µM (Fig. 1E, Table 1), thus validating the STR activity of the fusion. Our results demonstrate that CD-Rhd protein from *Pseudorhodoferax* is bifunctional having efficient dual activities using L-cysteine or thiosulfate as a sulfur donor. The activity of one domain is not hampered by the presence of the second domain.

A. thaliana STR18 stimulates the cysteine desulfurase activity of ABA3

The results obtained with this chimeric protein prompted us to investigate the interaction between *Arabidopsis thaliana* orthologs that exist as separate proteins, focusing on the cytosolic ABA3 and STR18, a single Rhd-domain containing protein (22, 24, 30, 31). The ABA3 and STR18 proteins possess CD and TST activity respectively, as already described (19, 32). The turnover for cysteine desulfuration of ABA3 was found to be ~2-fold higher in the presence of STR18 (0.64 *vs* 1.25 mole sulfur mole enz^{-1} min^{-1}), indicating a stimulating effect of STR18 on the CD activity of ABA3 (Fig. 2A).

A truncated version of ABA3 devoid of the MOSC domain and thus containing only the CD domain (ABA3-CD) was expressed and the effect of STR18 on its capacity to catalyze cysteine desulfuration also assessed

(Fig. 2B-C, Table 2). In the absence of STR18, the apparent K_m values of ABA3 and ABA3-CD for L-cysteine were 30 ± 4 µM and 59 ± 7 µM respectively and the deduced catalytic efficiencies were 520 M^{-1} s^{-1} and 850 M^{-1} s^{-1}, respectively (Fig. 2B-C, Table 2). These results confirmed that the N-terminal CD domain of ABA3 is sufficient to support CD activity and were in accordance with the previous *in vitro* characterization of ABA3-CD which reported an apparent K_m value of 50 µM for L-cysteine (19, 21). In the presence of STR18, ABA3 was 5-fold more efficient (k_{cat}/K_m of 2.8 x 10^3 M^{-1} s^{-1}) and this is notably explained by a decrease of the apparent K_m value for L- cysteine (8 ± 2 µM) by a factor of 3 (Fig. 2B, Table 2). On the contrary, STR18 did not significantly increase the catalytic efficiency (1.1 x 10^3 M^{-1} s^{-1}) of ABA-CD because the apparent K_m value for L-cysteine (99 ± 22 µM) was increased by a factor 2 (Fig. 2C, Table 2). Altogether, these data indicate that STR18 stimulates the CD activity of full-length ABA3 by increasing ABA3 affinity for L-cysteine. To further characterize ABA3-STR18 interaction, the CD activity of ABA3 and ABA-CD was monitored in the presence of 500 µM L-cysteine and of increasing STR18 concentrations. This allowed us to determine apparent K_m values of ABA3 and ABA3-CD for STR18 of 1.1 ± 0.3 and 1.7 ± 0.9 µM respectively (Fig. 3, Table 2, Fig. S1). These K_m values in the low micromolar range indicate that the ABA3-STR18 interaction may be physiologically relevant.

STR18 is persulfidated upon reaction with ABA3

As L-cysteine is not a sulfur donor for STR18 (Fig. S2), we assumed that STR18 stimulated ABA3 activity by reducing the persulfide formed on ABA3 more efficiently than the reductants used in the activity assay. In other words, this implied the transfer of sulfur atoms from ABA3 to STR18. To validate the formation of a persulfidated STR18, we analyzed by mass spectrometry the molecular mass of STR18 before and after incubation with a catalytic amount of ABA3 and an excess of L-cysteine in the absence of reductant. An increase of the molecular mass of STR18 by 31.3 Da, likely corresponding to a sulfur atom, was observed after this reaction as compared with a pre-reduced STR18. As this mass difference disappeared after a DTT treatment, we concluded that STR18 was mono-persulfidated upon reaction with ABA3 in the presence of L-cysteine (Table 3, Fig. S3).

STR18 possesses two cysteine residues, Cys47 and Cys89, the latter corresponding to the catalytic cysteine found in the CxxGxR signature typical of the Rhd domain (24, 31). A TST activity assay was performed with STR18 and both C47S and C89S variants. The STR18 C89S variant was totally inactive whereas the activity of the STR18 C47S variant was only marginally affected (Fig. 4, Table 4). This confirmed that STR18 exhibits TST activity, that Cys89 is mandatory and Cys47 dispensable.

To firmly establish which cysteine of STR18 is persulfidated by ABA3, similar incubation of STR18 variants with ABA3 and L-cysteine have been performed and analyzed by mass spectrometry. A DTT-reversible increase of *ca* 32 Da was detected for the C47S variant but not the C89S variant (Table 3, Fig. S4, S5). This indicated that STR18 was persulfidated on Cys89. Altogether, these data demonstrated the persulfidation of the Cys89 of STR18 by ABA3 in the presence of L-cysteine and the dispensable role of Cys47 for both the TST activity and the ABA3-related persulfidation of STR18. Furthermore, these results also suggest that STR18 can be persulfidated in the absence of reductant/sulfur acceptor raising the question of the physiological acceptors.

STR18 promotes trans-persulfidation reaction between two proteins

In the absence of a known sulfur acceptor(s) for STR18, we have investigated the capability of STR18 to transfer a sulfur atom to a protein substrate by using roGFP2 which was previously used to monitor persulfide generation in living cells (33). We have thus tested the oxidation of a pre-reduced roGFP2 in the presence of STR18 and thiosulfate (Fig. 5A). Whereas thiosulfate alone had no effect, the addition of STR18 promoted roGFP2 oxidation (Fig. 5A). This result validated a trans-persulfidation reaction between thiosulfate, the catalytic Cys89 of STR18 and roGFP2. Then, we investigated roGFP2 oxidation by STR18 in the presence of ABA3 and L-cysteine instead of thiosulfate (Fig. 5B). We have first verified that STR18 or ABA3 alone did not oxidize roGFP2 with L-cysteine. These results confirmed that L-

cysteine is not a sulfur donor for STR18 and validated that ABA3 is unable to promote roGFP2 oxidation. On the contrary, roGFP2 was oxidized by the whole system (L-cysteine, ABA3, STR18). These results demonstrated that STR18 mediates the sulfur transfer from ABA3 to roGFP2 catalyzing a trans-persulfidation reaction between both proteins.

DISCUSSION

In plants, CDs are key enzymes involved in the maturation of both Fe-S- and Moco-containing proteins (14, 15, 19). As CDs act in the early steps of the maturation process and these metalloproteins fulfill important roles, the deletion of CD encoding genes in plants is generally lethal or strongly affects development (14, 15). Considering that CDs serve as a central hub for sulfur mobilization and subsequent transfer to various metabolic pathways in non-photosynthetic organisms, we postulate that the strong phenotypes of mutant plants have thus so far prevented the identification of other sulfur-dependent pathways in which CDs are involved.

The multiple properties of CD proteins are also evident from the existence of fusion proteins containing a CD domain associated to diverse protein domains. The plant ABA3 possesses a MOSC domain that linked the protein function with Moco maturation. According to the known interaction between *E. coli* IscS and the ThiI or YnjE sulfurtransferases (26, 27), CD-Rhd chimera exist in several bacteria. Here, we described that a *Pseudorhodoferax* CD-Rhd is a PLP containing-homodimer exhibiting a dual activity profile, as it catalyzes cysteine and thiosulfate desulfuration. It is noticeable that this *Pseudorhodoferax* CD-Rhd was the most efficient cysteine desulfurase characterized so far, with a rate of sulfide formation of 2800 nmol min^{-1} mg^{-1} in the presence of L-cysteine and DTT. This activity is between 8 and 250-fold higher as compared with bacterial (*A. vinelandii* NifS and IscS, *B. subtilis* SufS, *E. coli* IscS and SufS, *Erwinia chrysanthemi* SufS), and eukaryotic CDs *(A. thaliana* NFS2, human and yeast NFS1) (Table 5). This remains true if we consider the activity of group II CD members in the presence of their respective activators. Indeed, the rate of sulfide formation ranged from 550 nmol min^{-1} mg^{-1} for *A. thaliana* NFS2-SUFE1, to 750 and 900 nmol min^{-1} mg^{-1} for *E. chrysanthemi* and *E. coli* SufS-SUFE, respectively (Table 5) (11, 16). Hence, the presence of a C-terminal Rhd domain in such fusions does not prevent the formation of the homodimer characteristic of CD proteins (8) but rather increases its activity by likely acting as a sulfur acceptor as observed for group II CD isoforms and their specific activators. Moreover, *Pseudorhodoferax* CD-Rhd exhibited a TST activity indicating that the Rhd domain is also functional. It displayed a better affinity for thiosulfate as compared to *E. coli* TST isoforms, GlpE and PspE, ($K_{m,app}$ of 238 µM *vs* 78 mM and 2.7 mM) (34, 35) and a 3-fold higher catalytic efficiency than STR18 (Table 4). Hence, CD-Rhd is a bifunctional enzyme using both L-cysteine and thiosulfate as sulfur donors.

The existence of such natural fusion proteins prompted us to analyze whether the activity of ABA3 is enhanced by STR or in other words if a persulfide transfer reaction is possible between these proteins. In the presence of L-cysteine and DTT, both the full-length ABA3 and the ABA3-CD domain displayed a weak CD activity, with k_{cat} values in the range of the values reported for other CD isoforms (Table 5) (21). The removal of the MOSC domain had mild effect, decreasing the affinity for L-cysteine by a factor 2 but globally increasing the catalytic efficiency because of an effect on the k_{cat} of the reaction (Table 2). Concerning the impact of STR18, the catalytic efficiency of ABA3 increased 5-fold in the presence of STR18, an effect mostly due to a change in affinity for L-Cys (4-fold lower apparent K_m value). Similar effects were reported for the plastidial SUFE1 protein which decreased by a factor 2 the K_m value of NFS2 for L-cysteine and increased 42-fold the rate of sulfide formation by NFS2 (16). Furthermore, the low K_m value of 1 µM of ABA3 for STR18 determined under steady-state conditions is consistent with the values obtained for the *B. subtilis* SufS-SufU and *E. coli* SufS-SufE couples (Table 5) (13, 36, 37). Interestingly, in all these examples the apparent K_m values of the CDs for their protein partners are lower than their apparent K_m values for L-cysteine (8-fold lower for ABA3-STR18 and 20-fold lower for *B. subtilis* SufS-SufU and *E. coli* SufS-SufE couples) (13, 36, 37). Hence, all these results suggest the existence of a highly specific ABA-STR18 interaction *via* the CD domain of ABA3.

Both the TST activity and the positive effect on ABA3 activity of STR18 underlined the ability of STR18 to form an intermediate persulfide as demonstrated previously for *A. vinelandii* Rhd isoform RhdA in the presence of *E. coli* IscS (38). This was also expected from the sulfur transfer observed from *E. coli* SufS and CsdA to SufE and CsdE respectively (10, 39). The ABA3-dependent persulfidation of the catalytic Cys89 of STR18 was indeed demonstrated by mass spectrometry after incubation of pre-reduced STR18 with both L-cysteine and ABA3 (Table 3). By accepting the sulfur atom, STR18 somehow stimulates the CD activity of ABA3 and regenerates its active form as a persulfidated ABA3 no longer interacts with L-cysteine and displays CD activity (40). In the absence of known STR18 partner(s), we further demonstrated the capacity of STR18 to perform trans-persulfidation reactions from either thiosulfate or L-Cys and ABA3 to roGFP2 (Fig. 5). From the apparent K_m values of STR18 for thiosulfate (273 ± 38 µM) and of ABA3 for STR18 (1.1 ± 0.3 µM), and the ability of ABA3 to promote STR18 persulfidation more efficiently than thiosulfate, ABA3 may be seen as the preferential sulfur donor for STR18.

Interestingly, this sulfur transfer pathway from ABA3 to STR18 may be independent of a sulfur transfer to the MOCS domain and thus independent of MoCo sulfuration. In which physiological context such a pathway is relevant remains however to be demonstrated because other cytosolic STRs are found in Arabidopsis. In addition to STR18, *A. thaliana* possesses at least two other cytosolic STR isoforms, the MST isoform STR2 and the two domain-containing protein STR13 also referred to as CNX5/MOCS3 (24). Noteworthy, STR2 and STR13 are present in all eukaryotic photosynthetic organisms whereas STR18 is present only in dicotyledonous plants (24). The physiological function(s) of STR2 and STR18 are yet unknown unlike STR13 which possesses a dual function, delivering the sulfur needed for the thio-modification of cytosolic tRNAs and for Moco biosynthesis owing to its N-terminal domain (31, 41). In human cells, a cytosolic form of NFS1 (although its existence is debated) was proposed to provide sulfur to MOCS3 eventually involving a relay by TUM1, the ortholog of plant STR2 (28, 42, 43).

While similar actors are present in plants, it may be that this cytosolic sulfur trafficking pathway is different between human and plant cells. Indeed, *A. thaliana str2* mutant lines have no phenotype and *str13* mutants (*cnx5-1* and *cnx5-2*) exhibit a dwarf phenotype with slightly green and morphologically aberrant leaves (41, 44). On the contrary, *aba3* mutants (*aba3-1*, *aba3-2*, *los5-1*, *los5-2*, *aba3-7*, *aba3-8*) have distinct and less severe phenotypes (45–47) than *str13* mutants. This suggests either that STR13 persulfidation is independent from ABA3 or that STR13 possesses additional functions.

From our results, we propose that in addition to its role in the maturation of the Moco-containing proteins, XDH and AO, ABA3 acts as a sulfur donor to STR proteins (either STR18 as demonstrated here or other cytosolic members such as STR2). The trans-persulfidation pathway involving cysteine and an ABA3-STR couple might thus represent an uncharacterized sulfur trafficking pathway in the cytosol of plants.

EXPERIMENTAL PROCEDURES

Materials

3- MP (sodium salt) was purchased from Santa Cruz Biotechnology (Dallas, TX, USA), lead (II) acetate, L-cysteine, thiosulfate, GSH and β-mercaptoethanol were from Sigma-Aldrich (St Louis, MO, USA).

Cloning and site-directed mutagenesis

The sequences coding for *A. thaliana* STR18 (At5g66170), the full-length ABA3 (At1g16540) and its CD domain (aa1-506, ABA3-CD) were cloned into the *Nde*I and *Bam*HI restriction sites of pET15b. Both cysteine residues (Cys47 and Cys89) of STR18 were individually substituted into serines to generate pET15b-STR18 C47S and pET15b-STR18 C89S recombinant plasmids. A synthetic cDNA of *Pseudorhodoferax sp.* Leaf274 CD-Rhd fusion protein (WP_056898193.1) was codon-optimized for *E. coli* expression (Genecust) and cloned into the *Nde*I and *Bam*HI restriction sites of pET15b. All primers used in this study are listed in Table S1.

Heterologous expression in E. coli and purification of recombinant proteins

For protein expression, the *E. coli* BL21 (DE3), C41 (DE3) and Rosetta2 (DE3) pLysS strains, were transformed respectively with pET15b At*STR18*, At*ABA3* or At*ABA3-CD* and *Pseudorhodoferax* CD-Rhd. The BL21 (DE3) and C41 (DE3) strains also contained the pSBET plasmid which allows expression of the tRNA needed to recognize the AGG and AGA rare codons. Cell cultures were successively amplified up to 2.4 l, for STR18, STR18 C47S, STR18 C89S and CD-Rhd, and 4.8 l for ABA3 and ABA3-CD, in LB medium supplemented with 50 µg/ml of ampicillin and kanamycin for BL21 and C41 strains or with 50 µg/ml of ampicillin and 34 µg/ml of chloramphenicol for Rosetta2 strain and grown at 37°C. STR18 expression was induced at exponential phase by adding 100 µM isopropyl β-D-thiogalactopyranoside (IPTG) for 4 h at 37°C. For ABA3, ABA3-CD and CD-Rhd, the culture protocol was modified. At exponential phase, the cultures were supplemented with ethanol 0.5% (v:v) and 100 µM pyridoxine hydrochloride and placed at 4°C for 2 h. Protein expression was then induced by adding 100 µM IPTG for 18 h at 20°C. After centrifugation (20 min at 6,380 x g), the cell pellets were resuspended in about 20 ml of 50 mM Tris-HCl pH 8.0, 300 mM NaCl, 10 mM imidazole buffer and stored at -20°C.

Cell lysis was completed by sonication (3 x 1 min with intervals of 1 min) and the soluble and insoluble fractions were separated by centrifugation for 30 min at 27,216 x g. For all proteins, the soluble fraction was loaded on Ni^{2+} affinity column (Sigma-Aldrich, St Louis MO, USA). After extensive washing, proteins were eluted by a 50 mM Tris-HCl pH 8.0, 300 mM NaCl, 250 mM imidazole buffer. The recombinant proteins were concentrated by ultrafiltration under nitrogen pressure and dialyzed (Amicon, YM10 membrane), and finally stored in a 30 mM Tris-HCl pH 8.0, 200 mM NaCl buffer supplemented with 5 mM DTT and 50% glycerol at -20°C. Protein concentrations were determined spectrophotometrically using a molecular extinction coefficient at 280 nm of 11,585 M^{-1} cm^{-1} for STR18 and 11,460 M^{-1} cm^{-1} for its monocysteinic variants, 97,845 M^{-1} cm^{-1} and 57,800 M^{-1} cm^{-1}, for ABA3 and ABA3-CD, and 47,690 M^{-1} cm^{-1} for CD-Rhd, respectively. The roGFP2 recombinant protein used in this study has been purified as described previously (51).

Determination of the oligomerization state of CD-Rhd

The oligomerization state of CD-Rhd was analyzed by size-exclusion chromatography as described previously (52). The detection was recorded by measuring absorbances at 280 and 418 nm.

Cysteine desulfurase activity assays

The CD activity was assayed at 25°C in a final volume of 400 µl of 30 mM Tris-HCl pH 8.0 buffer, 10 µM PLP, 5 mM reductant (DTT, GSH or β-mercaptoethanol) and 25 nM CD-Rhd, 1 µM ABA3 or 1 µM ABA3-CD. To assess the impact of STR18 on ABA3 activity, 5 µM STR18 was added in the reaction mixture. The reaction was initiated by adding L-cysteine and stopped after 30 min by adding 50 µl of 20 mM N,N-dimethyl-p-phenylenediamine dihydrochloride (DMPD, prepared in 7.2 M HCl). The addition of 50 µl of 30 mM $FeCl_3$ (prepared in 1.2 M HCl), followed by a 20 min incubation led to formation of methylene blue, which was then measured at 670 nm. Sodium sulfide (Na_2S) in the range of 1 to 100 µM was used for standard curve calibration.

Thiosulfate sulfurtransferase activity assays

The thiosulfate sulfurtransferase activity of CD-Rhd was assayed at 25°C in a final volume of 500 µl of 30 mM Tris-HCl pH 8.0 buffer, 5 mM β-mercaptoethanol, 0.4 mM lead (II) acetate (Sigma-Aldrich, St Louis MO, USA), various concentrations of thiosulfate ranging from 0 to 7 mM and 100 nM CD-Rhd. The reaction was initiated by adding CD-Rhd. After 25 min, the subsequent formation of lead sulfide was determined spectrophotometrically using a molar extinction coefficient of 5,500 M^{-1} cm^{-1} at 390 nm.

The TST activity of STR18 and its monocysteinic variants was monitored by detecting the produced H_2S using the methylene blue assay as described in the "Cysteine desulfurase activity assays" section. In a final volume of 400 µl of 30 mM Tris-HCl pH 8.0, 200 mM NaCl buffer, the reaction mixture contained 250 µM thiosulfate, 1 mM DTT and 50 nM STR18 added to start the reaction which was stopped after 15 min at 25°C.

Detection of persulfidated STR18 by mass spectrometry

In a final volume of 150 µl of 30 mM Tris HCl pH 8.0, 200 mM NaCl buffer, 150 µM of pre-reduced STR18, STR18 C47S and STR18 C89S were incubated 30 min in the presence of 300 µM L-cysteine, 2 µM ABA3 and 5 µM PLP at 25°C. After extensive dialysis, samples were split in two parts and treated or not with 1 mM DTT. Mass spectrometry analysis of these samples was performed using a Bruker microTOF-Q spectrometer (Bruker Daltonik, Bremen, Germany), equipped with Apollo II electrospray ionization source with ion funnel, operated in the negative ion mode. The concentrated samples in formic acid were injected at a flow rate of 10-20 µl min^{-1}. The potential between the spray needle and the orifice was set to 4.5 kV. Before each run the instrument was calibrated externally with the Tunemix™ mixture (Agilent Technologies) in quadratic regression mode. Data were analyzed with the DataAnalysis software (Bruker).

roGFP2 oxidation experiments

The capacity of ABA3 and STR18 to oxidize roGFP2 was analyzed *in vitro* by ratiometric time-course measurements on a Cary Eclipse spectrofluorimeter with excitation at 390 and 480 nm and detection of emitted fluorescence at 510 nm. The maximum oxidation and reduction of roGFP2 were defined using H_2O_2 and DTT concentrations of 10 mM. Pre-reduced roGFP2 was obtained by incubation with 10 mM DTT for 1 h and subsequent desalting on a G25 column to remove excess DTT. In a final volume of 400 µl of 30 mM Tris-HCl pH 8.0, 200 mM NaCl, the reaction mixtures contained 1 µM pre-reduced roGFP2 and either 5 mM thiosulfate and 5 µM STR18 or 1 mM L-cysteine, 10 µM PLP, 1 µM ABA3 and 5 µM STR18.

Acknowledgments

This work was supported by the Agence Nationale de la Recherche as part of the "Investissements d'Avenir" program (ANR-11-LABX-0002-01, Lab of Excellence ARBRE) and by grant no. ANR-16-CE20-0012. Technical support from Fabien Lachaud and François Dupire of the “Service Commun de Spectrométrie de Masse et Chromatographie” of the Université de Lorraine is gratefully acknowledged.

Conflict of interest

The authors declare no conflict of interest.

Author contributions

BS designed, performed and analyzed the experiments and wrote the manuscript. TD and MH performed some of the biochemical analyses. NR and JC supervised and helped conceiving the experiments, analyzed the data and wrote the manuscript.

REFERENCES

1. Mueller, E. G. (2006) Trafficking in persulfides: delivering sulfur in biosynthetic pathways. *Nat. Chem. Biol.* **2**, 185–194
2. Behshad, E., and Bollinger, J. M. (2009) Kinetic analysis of cysteine desulfurase CD0387 from Synechocystis sp. PCC 6803: formation of the persulfide intermediate. *Biochemistry*. **48**, 12014–12023
3. Zheng, L., White, R. H., Cash, V. L., Jack, R. F., and Dean, D. R. (1993) Cysteine desulfurase activity indicates a role for NIFS in metallocluster biosynthesis. *Proc. Natl. Acad. Sci. U. S. A.* **90**, 2754–2758
4. Zheng, L., Cash, V. L., Flint, D. H., and Dean, D. R. (1998) Assembly of iron-sulfur clusters identification of an iscSUA-hscBA-fdx gene cluster from Azotobacter vinelandii. *J. Biol. Chem.* **273**, 13264–13272
5. Patzer, S. I., and Hantke, K. (1999) SufS is a NifS-like protein, and SufD is necessary for stability of the [2Fe-2S] FhuF protein in Escherichia coli. *J. Bacteriol.* **181**, 3307–3309
6. Mihara, H., and Esaki, N. (2002) Bacterial cysteine desulfurases: their function and mechanisms. *Appl. Microbiol. Biotechnol.* **60**, 12–23
7. Shi, R., Proteau, A., Villarroya, M., Moukadiri, I., Zhang, L., Trempe, J.-F., Matte, A., Armengod, M. E., and Cygler, M. (2010) Structural Basis for Fe–S Cluster Assembly and tRNA

Thiolation Mediated by IscS Protein–Protein Interactions. *PLoS Biol.* 10.1371/journal.pbio.1000354

8. Roret, T., Pégeot, H., Couturier, J., Mulliert, G., Rouhier, N., and Didierjean, C. (2014) X-ray structures of Nfs2, the plastidial cysteine desulfurase from Arabidopsis thaliana. *Acta Crystallogr. Sect. F Struct. Biol. Commun.* **70**, 1180–1185
9. Black, K. A., and Dos Santos, P. C. (2015) Shared-intermediates in the biosynthesis of thio-cofactors: Mechanism and functions of cysteine desulfurases and sulfur acceptors. *Biochim. Biophys. Acta*. **1853**, 1470–1480
10. Outten, F. W., Wood, M. J., Munoz, F. M., and Storz, G. (2003) The SufE protein and the SufBCD complex enhance SufS cysteine desulfurase activity as part of a sulfur transfer pathway for Fe-S cluster assembly in Escherichia coli. *J. Biol. Chem.* **278**, 45713–45719
11. Loiseau, L., Ollagnier-de-Choudens, S., Nachin, L., Fontecave, M., and Barras, F. (2003) Biogenesis of Fe-S cluster by the bacterial Suf system: SufS and SufE form a new type of cysteine desulfurase. *J. Biol. Chem.* **278**, 38352–38359
12. Loiseau, L., Ollagnier-de Choudens, S., Lascoux, D., Forest, E., Fontecave, M., and Barras, F. (2005) Analysis of the heteromeric CsdA-CsdE cysteine desulfurase, assisting Fe-S cluster biogenesis in Escherichia coli. *J. Biol. Chem.* **280**, 26760–26769
13. Selbach, B., Earles, E., and Dos Santos, P. C. (2010) Kinetic analysis of the bisubstrate cysteine desulfurase SufS from Bacillus subtilis. *Biochemistry*. **49**, 8794–8802
14. Frazzon, A. P. G., Ramirez, M. V., Warek, U., Balk, J., Frazzon, J., Dean, D. R., and Winkel, B. S. J. (2007) Functional analysis of Arabidopsis genes involved in mitochondrial iron-sulfur cluster assembly. *Plant Mol. Biol.* **64**, 225–240
15. Van Hoewyk, D., Abdel-Ghany, S. E., Cohu, C. M., Herbert, S. K., Kugrens, P., Pilon, M., and Pilon-Smits, E. A. H. (2007) Chloroplast iron-sulfur cluster protein maturation requires the essential cysteine desulfurase CpNifS. *Proc. Natl. Acad. Sci. U. S. A.* **104**, 5686–5691
16. Ye, H., Abdel-Ghany, S. E., Anderson, T. D., Pilon-Smits, E. A. H., and Pilon, M. (2006) CpSufE activates the cysteine desulfurase CpNifS for chloroplastic Fe-S cluster formation. *J. Biol. Chem.* **281**, 8958–8969
17. Murthy, N. M. U., Ollagnier-de-Choudens, S., Sanakis, Y., Abdel-Ghany, S. E., Rousset, C., Ye, H., Fontecave, M., Pilon-Smits, E. A. H., and Pilon, M. (2007) Characterization of Arabidopsis thaliana SufE2 and SufE3: functions in chloroplast iron-sulfur cluster assembly and Nad synthesis. *J. Biol. Chem.* **282**, 18254–18264
18. Xu, X. M., and Møller, S. G. (2006) AtSufE is an essential activator of plastidic and mitochondrial desulfurases in Arabidopsis. *EMBO J.* **25**, 900–909
19. Bittner, F., Oreb, M., and Mendel, R. R. (2001) ABA3 is a molybdenum cofactor sulfurase required for activation of aldehyde oxidase and xanthine dehydrogenase in Arabidopsis thaliana. *J. Biol. Chem.* **276**, 40381–40384
20. Kaufholdt, D., Baillie, C.-K., Meyer, M. H., Schwich, O. D., Timmerer, U. L., Tobias, L., van Thiel, D., Hänsch, R., and Mendel, R. R. (2016) Identification of a protein-protein interaction network downstream of molybdenum cofactor biosynthesis in Arabidopsis thaliana. *J. Plant Physiol.* **207**, 42–50
21. Heidenreich, T., Wollers, S., Mendel, R. R., and Bittner, F. (2005) Characterization of the NifS-like domain of ABA3 from Arabidopsis thaliana provides insight into the mechanism of molybdenum cofactor sulfuration. *J. Biol. Chem.* **280**, 4213–4218
22. Wollers, S., Heidenreich, T., Zarepour, M., Zachmann, D., Kraft, C., Zhao, Y., Mendel, R. R., and Bittner, F. (2008) Binding of sulfurated molybdenum cofactor to the C-terminal domain of ABA3 from Arabidopsis thaliana provides insight into the mechanism of molybdenum cofactor sulfuration. *J. Biol. Chem.* **283**, 9642–9650
23. Bordo, D., and Bork, P. (2002) The rhodanese/Cdc25 phosphatase superfamily. Sequence-structure-function relations. *EMBO Rep.* **3**, 741–746
24. Moseler, A., Selles, B., Rouhier, N., and Couturier, J. (2019) Novel insights into the diversity of the sulfurtransferase family in photosynthetic organisms with emphasis on oak. *New Phytol.* 10.1111/nph.15870
25. Cipollone, R., Ascenzi, P., and Visca, P. (2007) Common themes and variations in the rhodanese superfamily. *IUBMB Life*. **59**, 51–59

26. Dahl, J.-U., Urban, A., Bolte, A., Sriyabhaya, P., Donahue, J. L., Nimtz, M., Larson, T. J., and Leimkühler, S. (2011) The identification of a novel protein involved in molybdenum cofactor biosynthesis in Escherichia coli. *J. Biol. Chem.* **286**, 35801–35812
27. Kambampati, R., and Lauhon, C. T. (2000) Evidence for the transfer of sulfane sulfur from IscS to ThiI during the in vitro biosynthesis of 4-thiouridine in Escherichia coli tRNA. *J. Biol. Chem.* **275**, 10727–10730
28. Fräsdorf, B., Radon, C., and Leimkühler, S. (2014) Characterization and interaction studies of two isoforms of the dual localized 3-mercaptopyruvate sulfurtransferase TUM1 from humans. *J. Biol. Chem.* **289**, 34543–34556
29. Noma, A., Sakaguchi, Y., and Suzuki, T. (2009) Mechanistic characterization of the sulfur-relay system for eukaryotic 2-thiouridine biogenesis at tRNA wobble positions. *Nucleic Acids Res.* **37**, 1335–1352
30. Bauer, M., Dietrich, C., Nowak, K., Sierralta, W. D., and Papenbrock, J. (2004) Intracellular Localization of Arabidopsis Sulfurtransferases. *Plant Physiol.* **135**, 916–926
31. Selles, B., Moseler, A., Rouhier, N., and Couturier, J. (2019) Rhodanese domain-containing sulfurtransferases: multifaceted proteins involved in sulfur trafficking in plants. *J. Exp. Bot.* **70**, 4139–4154
32. Henne, M., König, N., Triulzi, T., Baroni, S., Forlani, F., Scheibe, R., and Papenbrock, J. (2015) Sulfurtransferase and thioredoxin specifically interact as demonstrated by bimolecular fluorescence complementation analysis and biochemical tests. *FEBS Open Bio.* **5**, 832–843
33. Ezeriņa, D., Takano, Y., Hanaoka, K., Urano, Y., and Dick, T. P. (2018) N-Acetyl Cysteine Functions as a Fast-Acting Antioxidant by Triggering Intracellular H2S and Sulfane Sulfur Production. *Cell Chem. Biol.* **25**, 447-459.e4
34. Cheng, H., Donahue, J.L., Battle, S.E., Ray, W.K., and Larson, T.J. (2008) Biochemical and Genetic Characterization of PspE and GlpE, Two Single-domain Sulfurtransferases of Escherichia coli. *Open Microbiol. J.* **2**,18-28
35. Ray, W. K., Zeng, G., Potters, M. B., Mansuri, A. M., and Larson, T. J. (2000) Characterization of a 12-Kilodalton Rhodanese Encoded by glpE of Escherichia coli and Its Interaction with Thioredoxin. *J. Bacteriol.* **182**, 2277–2284
36. Albrecht, A. G., Peuckert, F., Landmann, H., Miethke, M., Seubert, A., and Marahiel, M. A. (2011) Mechanistic characterization of sulfur transfer from cysteine desulfurase SufS to the iron-sulfur scaffold SufU in Bacillus subtilis. *FEBS Lett.* **585**, 465–470
37. Dai, Y., and Outten, F. W. (2012) The E. coli SufS-SufE sulfur transfer system is more resistant to oxidative stress than IscS-IscU. *FEBS Lett.* **586**, 4016–4022
38. Forlani, F., Cereda, A., Freuer, A., Nimtz, M., Leimkühler, S., and Pagani, S. (2005) The cysteine-desulfurase IscS promotes the production of the rhodanese RhdA in the persulfurated form. *FEBS Lett.* **579**, 6786–6790
39. Ollagnier-de-Choudens, S., Lascoux, D., Loiseau, L., Barras, F., Forest, E., and Fontecave, M. (2003) Mechanistic studies of the SufS-SufE cysteine desulfurase: evidence for sulfur transfer from SufS to SufE. *FEBS Lett.* **555**, 263–267
40. Lehrke, M., Rump, S., Heidenreich, T., Wissing, J., Mendel, R. R., and Bittner, F. (2012) Identification of persulfide-binding and disulfide-forming cysteine residues in the NifS-like domain of the molybdenum cofactor sulfurase ABA3 by cysteine-scanning mutagenesis. *Biochem. J.* **441**, 823–839
41. Nakai, Y., Harada, A., Hashiguchi, Y., Nakai, M., and Hayashi, H. (2012) Arabidopsis molybdopterin biosynthesis protein Cnx5 collaborates with the ubiquitin-like protein Urm11 in the thio-modification of tRNA. *J. Biol. Chem.* **287**, 30874–30884
42. Marelja, Z., Stöcklein, W., Nimtz, M., and Leimkühler, S. (2008) A novel role for human Nfs1 in the cytoplasm: Nfs1 acts as a sulfur donor for MOCS3, a protein involved in molybdenum cofactor biosynthesis. *J. Biol. Chem.* **283**, 25178–25185
43. Marelja, Z., Mullick Chowdhury, M., Dosche, C., Hille, C., Baumann, O., Löhmannsröben, H.-G., and Leimkühler, S. (2013) The L-cysteine desulfurase NFS1 is localized in the cytosol where it provides the sulfur for molybdenum cofactor biosynthesis in humans. *PloS One*. **8**, e60869

44. Mao, G., Wang, R., Guan, Y., Liu, Y., and Zhang, S. (2011) Sulfurtransferases 1 and 2 play essential roles in embryo and seed development in Arabidopsis thaliana. *J. Biol. Chem.* **286**, 7548–7557
45. Xiong, L., Ishitani, M., Lee, H., and Zhu, J. K. (2001) The Arabidopsis LOS5/ABA3 locus encodes a molybdenum cofactor sulfurase and modulates cold stress- and osmotic stress-responsive gene expression. *Plant Cell*. **13**, 2063–2083
46. Zhong, R., Thompson, J., Ottesen, E., and Lamppa, G. K. (2010) A forward genetic screen to explore chloroplast protein import in vivo identifies Moco sulfurase, pivotal for ABA and IAA biosynthesis and purine turnover. *Plant J.* **63**, 44–59
47. Watanabe, S., Sato, M., Sawada, Y., Tanaka, M., Matsui, A., Kanno, Y., Hirai, M. Y., Seki, M., Sakamoto, A., and Seo, M. (2018) Arabidopsis molybdenum cofactor sulfurase ABA3 contributes to anthocyanin accumulation and oxidative stress tolerance in ABA-dependent and independent ways. *Sci. Rep.* **8**, 16592
48. Mihara, H., Kurihara, T., Yoshimura, T., and Esaki, N. (2000) Kinetic and mutational studies of three NifS homologs from Escherichia coli: mechanistic difference between L-cysteine desulfurase and L-selenocysteine lyase reactions. *J. Biochem. (Tokyo)*. **127**, 559–567
49. Li, K., Tong, W.-H., Hughes, R. M., and Rouault, T. A. (2006) Roles of the Mammalian Cytosolic Cysteine Desulfurase, ISCS, and Scaffold Protein, ISCU, in Iron-Sulfur Cluster Assembly. *J. Biol. Chem.* **281**, 12344–12351
50. Mühlenhoff, U., Balk, J., Richhardt, N., Kaiser, J. T., Sipos, K., Kispal, G., and Lill, R. (2004) Functional characterization of the eukaryotic cysteine desulfurase Nfs1p from Saccharomyces cerevisiae. *J. Biol. Chem.* **279**, 36906–36915
51. Meyer, A. J., Brach, T., Marty, L., Kreye, S., Rouhier, N., Jacquot, J.-P., and Hell, R. (2007) Redox-sensitive GFP in Arabidopsis thaliana is a quantitative biosensor for the redox potential of the cellular glutathione redox buffer. *Plant J.* **52**, 973–986
52. Zannini, F., Roret, T., Przybyla-Toscano, J., Dhalleine, T., Rouhier, N., and Couturier, J. (2018) Mitochondrial Arabidopsis thaliana TRXo Isoforms Bind an Iron−Sulfur Cluster and Reduce NFU Proteins In Vitro. *Antioxidants* **7**, 142

Table 1. Kinetic parameters of cysteine desulfurase and thiosulfate sulfurtransferase activities of CD-Rhd.

Donor	Reductant	K_m (μM)	k_{cat} (s^{-1})	k_{cat}/K_m (M^{-1} s^{-1})
L-cysteine	DTT	238 ± 26	2.5 ± 0.1	1.1 x 10^4
L-cysteine	GSH	1,400 ± 297	2.1 ± 0.2	1.5 x 10^3
L-cysteine	β-ME	574 ± 54	3.0 ± 0.1	5.2 x 10^3
Thiosulfate	β-ME	331 ± 70	1.8 ± 0.1	5.4 x 10^3

The apparent K_m and turnover values (k_{cat}) were calculated by non-linear regression using the Michaelis-Menten equation. The data are represented as mean ± SD of three independent experiments.

Table 2. Kinetic parameters of cysteine desulfurase activity of the full-length ABA3 and its CD domain.

	K_m (μM)	k_{cat} (s^{-1})	k_{cat}/K_m (M^{-1} s^{-1})
		L-cysteine	
ABA3	30 ± 4	0.016 ± 0.001	5.2×10^2
ABA3-CD	59 ± 7	0.050 ± 0.001	8.5×10^2
ABA3 + STR18	8 ± 2	0.023 ± 0.001	2.8×10^3
ABA3-CD + STR18	99 ± 22	0.111 ± 0.007	1.1×10^3
		STR18	
ABA3	1.1 ± 0.3	0.006 ± 0.001	5.4×10^3
ABA3-CD	1.7 ± 0.9	0.006 ± 0.001	3.5×10^3

The CD activity of ABA3 and ABA3-CD was monitored in the presence of varying concentrations of L-cysteine and with or without STR18 as described in the "Experimental procedures" section. The apparent K_m and turnover values (k_{cat}) were calculated by non-linear regression using the Michaelis-Menten equation. The data are represented as mean ± SD of three independent experiments.

Table 3. Electrospray ionization mass spectrometry analysis of the redox state of STR18 and its monocysteinic variants.

Protein	Theoretical mass (Da)	Theoretical mass without Met (Da)	Pre-reduced with DTT	Treatment with ABA3 and L-cysteine	Δ mass (Da)
STR18	17,117.0	16,985.8	16,985.4	17,016.7	31.3
STR18 C47S	17,100.9	16,969.8	16,968.2	17,001.2	33.0
STR18 C89S	17,100.9	16,969.8	16,970.0	16,969.0	-1.0

Reduced proteins and proteins incubated with L-cysteine and ABA3 were analyzed by mass spectrometry. The mass accuracy is generally ± 0.5-1 Da. Note that the mass decrease of *ca* 131 Da compared to the theoretical molecular masses indicated that the methionine was cleaved off in *E. coli* (Table 3, Figs. S3-S5).

Table 4. Kinetic parameters of thiosulfate sulfurtransferase activity of STR18, C47S and C89S variants.

	K_m (µM)	k_{cat} (s^{-1})	k_{cat}/K_m (M^{-1} s^{-1})
		L-cysteine	
STR18	273 ± 38	0.48 ± 0.02	1.8 x 10^3
STR18 C47S	332 ± 47	0.42 ± 0.01	1.3 x 10^3
STR18 C89S	n.d.	n.d.	n.d.

The TST activity of STR18, C47S and C89S variants was monitored in the presence of varying concentrations of thiosulfate as described in the "Experimental procedures" section. The apparent K_m and turnover values (k_{cat}) were calculated by non-linear regression using the Michaelis-Menten equation. The data are represented as mean ± SD of three independent experiments. n.d. is not detected.

Table 5. Catalytic properties of characterized CD isoforms from various organisms.

Protein name	Organism	Activity (*nmol per min per mg*)	K_m cysteine (µM)	K_m acceptor (µM)	Reference
NifS	*Azotobacter vinelandii*	168	-	-	(4)
IscS	*Azotobacter vinelandii*	124	-	-	(4)
SufS	*Bacillus subtilis*	7	-	-	(13
SufS-SufU	*Bacillus subtilis*	240[a]	86	3	(13)
SufS	*Bacillus subtilis*				(36)
SufS-SufU	*Bacillus subtilis*	153.5	49.7	-	(36)
SufS-SufU	*Bacillus subtilis*	93.4	-	2.6	(36)
SufS	*Erwinia chrysanthemi*	21	-	-	(11)
SufS-SufE	*Erwinia chrysanthemi*	750	-	-	(11)
CsdA	*Escherichia coli*	1.2	140	-	(12)
CsdA-CsdE	*Escherichia coli*	2.5	540	-	(12)
IscS	*Escherichia coli*	51.7[b]	-	-	(37)
IscS	*Escherichia coli*	312.8[c]	-	-	(37)
IscS	*Escherichia coli*	380	-	-	(48)
SufS	*Escherichia coli*	19	-	-	(48)
SufS	*Escherichia coli*	19	-	-	(11)
SufS-SufE	*Escherichia coli*	900	-	-	(11)
SufS	*Escherichia coli*	25	-	-	(39)
SufS-SufE	*Escherichia coli*	700	-	-	(39)
SufS	*Escherichia coli*	2.6[b]	-	-	(37)
		7.9[c]	-	-	(37)
SufS-SufE	*Escherichia coli*	54.3	43.5	-	(37)
SufS-SufE	*Escherichia coli*	85.4	-	1.9	(37)
CD-Rhd	*Pseudorhodoferax*	2800	238	-	This study
NFS1	*Homo sapiens*	6.4	-	-	(49)
NFS1-ISD11	*Homo sapiens*		435		(42)
NFS1	*Saccharomyces cerevisiae*	12.7	-	-	(50)
NFS2	*Arabidopsis thaliana*	13	100	-	(16)
NFS2-SUFE1	*Arabidopsis thaliana*	550	43	-	(16)

[a] SufS-SufU activity with 10-fold excess of SufU

[b] SufS activity with 2 mM L-cysteine and 2 mM DTT

[c] SufS activity with 12 mM L-cysteine and 50 mM DTT

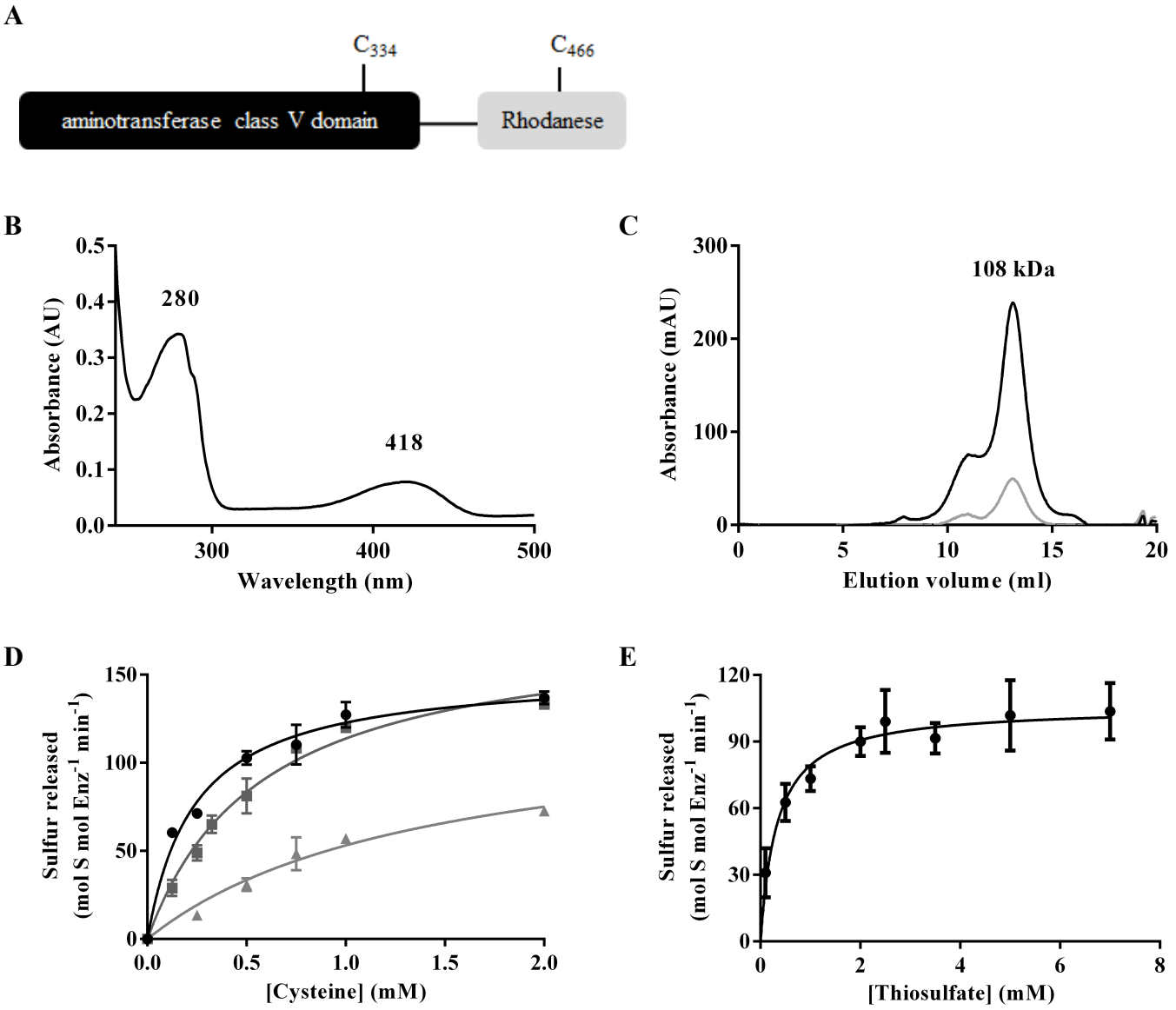

Figure 1. *Pseudorhodoferax* CD-Rhd fusion has a dual activity profile.

A. Modular organization of the Pseudorhodoferax CD-Rhd fusion (WP_056898193.1) presenting the position of the presumed catalytic cysteines of both CD and Rhd domains.

B. UV-visible absorption spectrum of the purified N-terminal His-tagged recombinant CD-Rhd recorded in a 30 mM Tris-HCl pH 8.0 buffer.

C. Analytical gel filtration (Superdex S200 10/300 column, GE Healthcare) of His-tagged recombinant CD-Rhd (100 µg). The presence of the polypeptide and of the PLP cofactor have been detected by measuring the absorbance at 280 nm (dark line) and 418 nm (grey line), respectively.

D. Steady-state kinetic parameters of the cysteine desulfurase activity. Reactions were performed in the presence of 25 nM CD-Rhd, increasing concentrations of cysteine (0 to 2 mM) and in the presence of various reductants, either 5 mM of DTT (black circles), or 5 mM GSH (grey triangles) or 5 mM β-mercaptoethanol (grey squares). The data are represented as mean ± SD of three independent experiments.

E. Steady-state kinetic parameters of the thiosulfate sulfurtransferase activity. Reactions were performed in the presence of 100 nM CD-Rhd, increasing concentrations of thiosulfate (0 to 7 mM) and 5 mM β-mercaptoethanol. The data are represented as mean ± SD of three independent experiments.

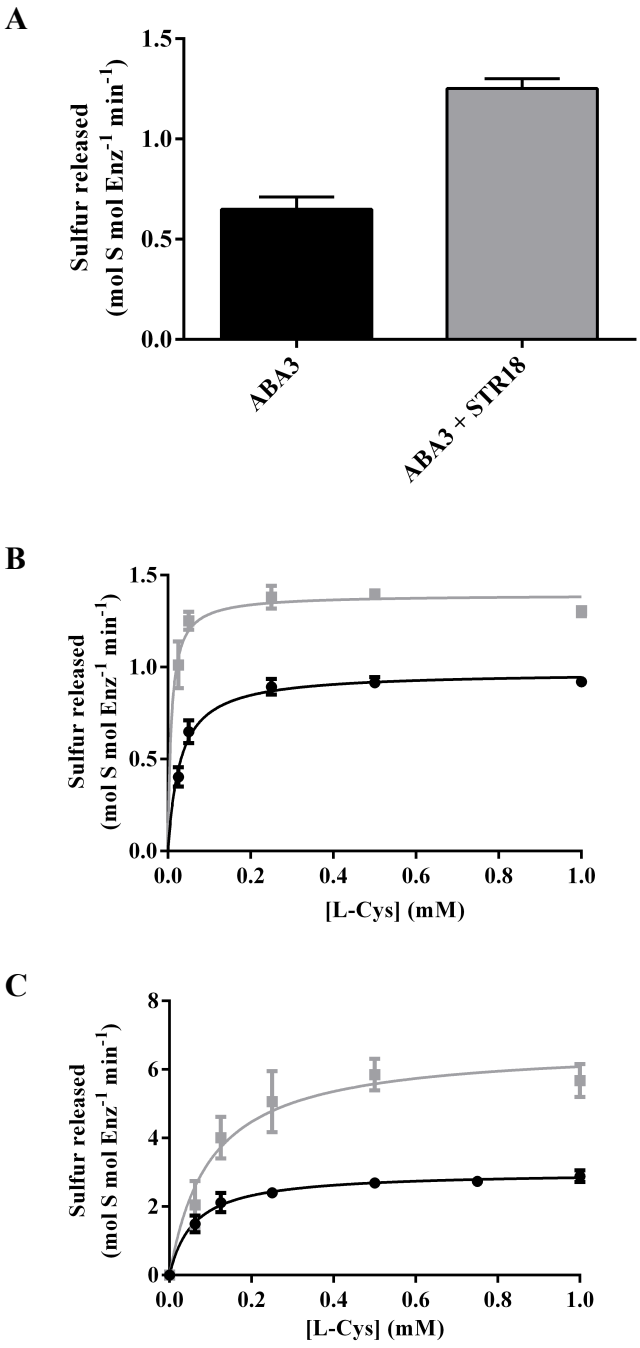

Figure 2. STR18 stimulates ABA3 activity.

A. Effect of STR18 on ABA3 cysteine desulfurase activity. CD activity was measured using 1 µM ABA3, 500 µM L-cysteine and 1 mM DTT in the presence or absence of 5 µM STR18. The data are represented as mean ± SD of three independent experiments.

B-C. Steady-state kinetic parameters of the CD activity of full-length ABA3 (B) and CD domain of ABA3 (ABA3-CD) (C) in the presence of L-cysteine and with (black circles) or without (grey squares) STR18. Activity was measured in the presence of 1 µM ABA3 or ABA3-CD, increasing concentrations of L-cysteine (0 to 1 mM), 5 mM DTT and 5 µM STR18 when present. The data are represented as mean ± SD of three independent experiments.

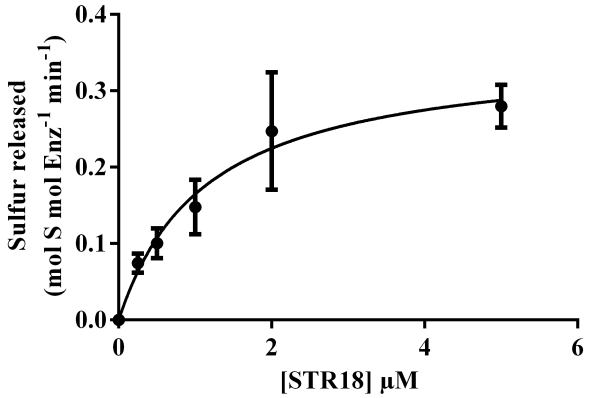

Figure 3. ABA3 possesses a relevant affinity for STR18.
Steady-state kinetic experiments to determine the apparent Km value of ABA3 for STR18 were performed by measuring the CD activity of 1 µM ABA3 in the presence of a fixed concentration of L-cysteine (500 µM), 5 mM DTT and increasing concentrations of STR18 (0 to 5 µM). The data are represented as mean ± SD of three independent experiments.

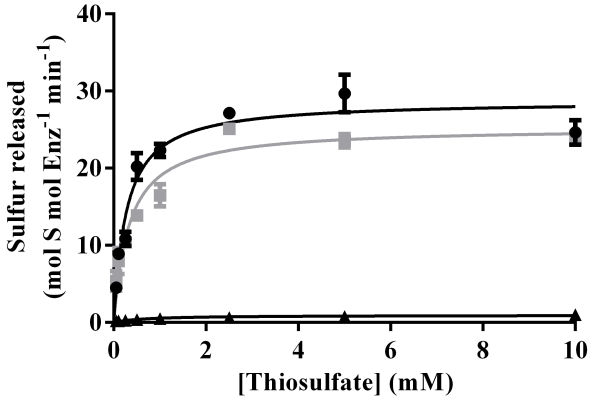

Figure 4. STR18 exhibits Cys89-dependent TST activity.
The TST activity of STR18 (black circles), STR18 C47S (grey squares) and STR18 C89S (black triangles) was measured under steady-state conditions using the lead acetate method in the presence of 100 nM STR18, 5 mM β-mercaptoethanol and increasing concentrations of thiosulfate (0 to 10 mM). The data are represented as mean ± SD of three independent experiments.

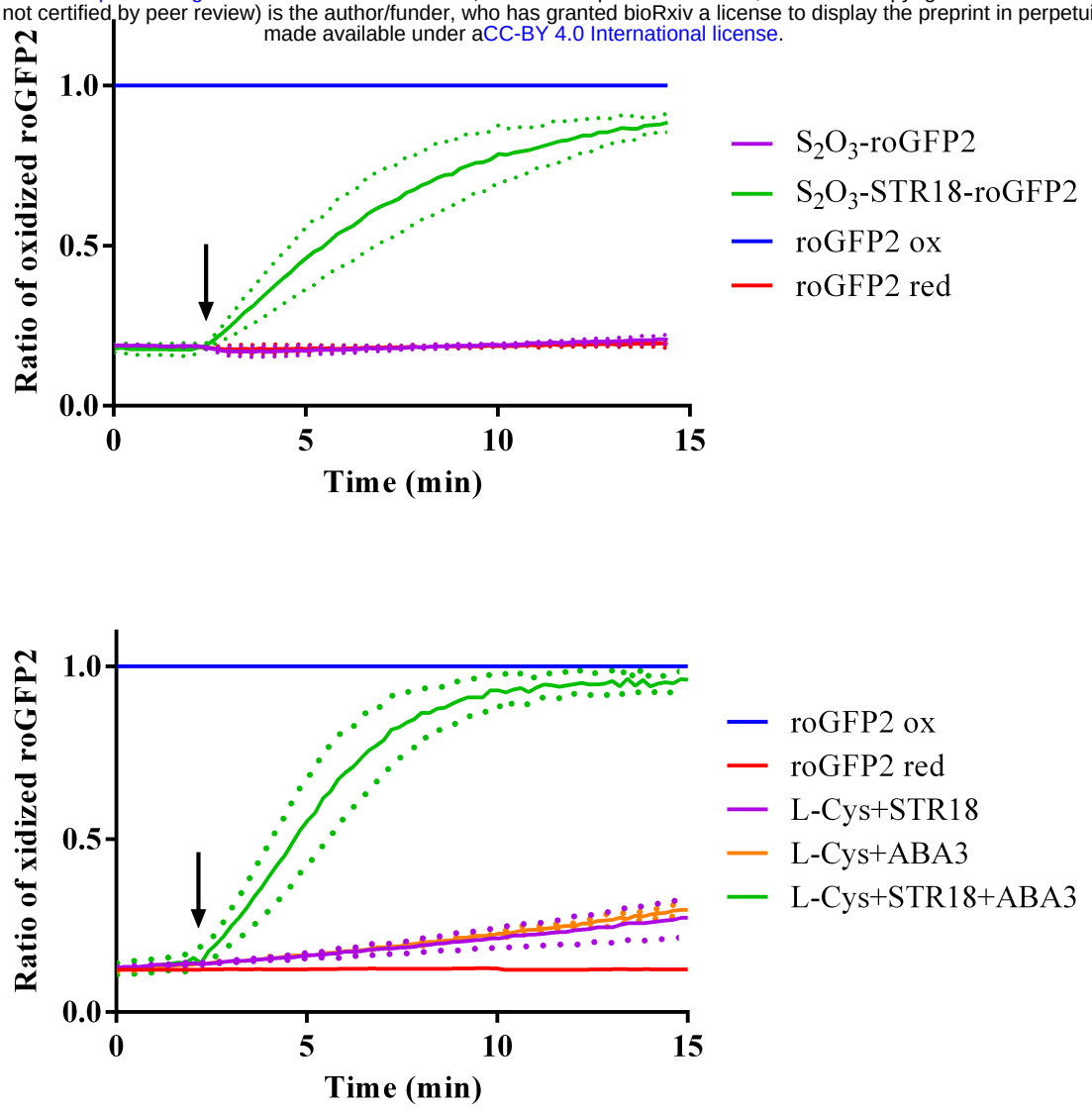

Figure 5. STR18 catalyzes the oxidation of roGFP2 via trans-persulfidation.
A. Persulfide-dependent oxidation kinetics of 1 µM roGFP2 in the presence of STR18 and thiosulfate.
B. Persulfide-dependent oxidation kinetics of 1 µM roGFP2 in the presence of L-Cys, ABA3 and STR18 or its cysteinic variants.
The arrows indicate the addition of STR18, if present. The fully reduced or oxidized roGFP2 used as references were obtained with 10 mM DTT or H_2O_2 respectively.